

Compressed Sensing with Shannon-Kotel'nikov Mapping in the Presence of Noise

Ahmad Abou Saleh, Wai-Yip Chan, and Fady Alajaji

Abstract—We propose a low delay/complexity sensor system based on the combination of Shannon-Kotel'nikov mapping and compressed sensing (CS). The proposed system uses a 1:2 nonlinear analog coder on the CS measurements in the presence of channel noise. It is shown that the purely-analog system, used in conjunction with either maximum a-posteriori or minimum mean square error decoding, outperforms the following reference systems in terms of signal-to-distortion ratio: 1) a conventional CS system that assumes noiseless transmission, and 2) a CS-based system which accounts for channel noise during signal reconstruction. The proposed system is also shown to be advantageous in requiring fewer sensors than the reference systems.

I. INTRODUCTION

With the increasing popularity of wireless sensors networks (WSNs), reliable transmission with delay and complexity constraints is more relevant than ever. Wireless sensor networking is a technology that monitors the physical world through a distributed network of wireless sensor nodes. These nodes, often conceived as having limited lifetime and processing power, communicate their sensed field information to a fusion center (FC). Communication takes place over power and bandwidth constrained noisy wireless channels [1]. To meet these challenges, in this paper, we investigate using low delay/complexity source-channel mapping with compressed sensing (CS) in WSNs.

The sensor inputs are treated as samples from an analog source. The traditional approach for analog source transmission is to use separate digital source and channel coders. This separation is optimal from a theoretical perspective [2]. In such systems, the analog source is encoded using a powerful vector quantizer, and capacity approaching channel codes, such as turbo or low-density-parity-check codes, are used for channel error protection. This approach results in very high delay and complexity, which is not desirable in WSNs. The approach used here is analog joint source-channel coding which has been shown to perform well under low delay and complexity constraints [3]–[7]. More specifically, we propose to use 1:2 Shannon-Kotel'nikov mappings within the CS context. The key idea is to use nonlinear dimension expansion, that acts as an analog joint source-channel encoder on the compressed

sensing measurements to increase their immunity against channel noise. In [8], a hybrid digital-analog system is used with distributed compressed sensing over noisy channels. In this paper, we consider a purely-analog system where all sensed and transmitted signals are analog-valued. For reference, we compare the proposed system with 1) a conventional CS system that assumes noiseless transmission, and 2) a CS-based system that accounts for channel noise during signal reconstruction [9]. The rest of the paper is organized as follows. In Section II, we briefly review the compressed sensing theory. Section III describes Shannon-Kotel'nikov mapping using the 1:2 double Archimedes' spiral. In Section IV, we develop the system structure and its optimization. Simulation results are included in Section V. Finally, conclusions are drawn in Section VI.

II. OVERVIEW OF COMPRESSED SENSING THEORY

The theory of compressed sensing has been developed in [9]–[11]. Specifically, it is shown that if $\mathbf{x} \in \mathbb{R}^N$ is a sparse signal in some basis Ψ with only K nonzero elements, then, with high probability, $M \geq CK \log_2(N/K)$ random linear measurements provide sufficient information for perfect signal reconstruction [9], where C is some positive constant. These linear measurements can be expressed as

$$\mathbf{y} = \Phi \mathbf{x} \quad (1)$$

where $\Phi \in \mathbb{R}^{M \times N}$ is a measurement matrix that is incoherent with the basis matrix Ψ (i.e. $\mu(\Psi, \Phi) \approx 1$, where $\mu(\Psi, \Phi)$ is the coherence which measures the largest correlation between any two elements of the basis and the measurement matrix) [12]. Knowing that the signal \mathbf{x} is sparse in some basis Ψ with transform coefficients \mathbf{u} ($\mathbf{x} = \Psi \mathbf{u}$), recovery of \mathbf{x} from the linear measurements \mathbf{y} can be done by solving the following convex optimization problem

$$\min_{\hat{\mathbf{x}}} \|\Psi^{-1} \hat{\mathbf{x}}\|_{\ell_1}, \quad \text{subject to } \Phi \hat{\mathbf{x}} = \mathbf{y} \quad (2)$$

where $\|(\cdot)\|_{\ell_1}$ is the ℓ_1 norm ($\|\mathbf{x}\|_{\ell_1} \triangleq \sum_{i=1}^N |x_i|$). Several optimization algorithms were developed to solve the ℓ_1 minimization problem such as basis pursuit (BP) [13], matching pursuit [14], and orthogonal matching pursuit [15].

In practice, the collected measurements are usually disturbed by noise \mathbf{n} ; thus \mathbf{y} is modeled as

$$\mathbf{y} = \Phi \mathbf{x} + \mathbf{n}. \quad (3)$$

For CS to be widely applicable, signal recovery should be robust against noise; a small disturbance in the measurements

This work was supported in part by NSERC of Canada.

A. Abou Saleh and W-Y. Chan are with the Department of Electrical and Computer Engineering, Queen's University, Kingston, ON, K7L 3N6, Canada.

F. Alajaji is with the Department of Mathematics and Statistics and the Department of Electrical and Computer Engineering, Queen's University, Kingston, ON, K7L 3N6, Canada.

should result in a small disturbance in the signal reconstruction. Using a noise-aware version of (2), the signal can be reconstructed as follows

$$\min_{\hat{\mathbf{x}}} \|\Psi^{-1}\hat{\mathbf{x}}\|_{\ell_1}, \quad \text{subject to } \|\Phi\hat{\mathbf{x}} - \mathbf{y}\|_2 \leq \epsilon \quad (4)$$

where ϵ bounds the total amount of noise in the measurements. Typically, the noise is assumed to be Gaussian $\mathbf{n} \sim \mathcal{N}(0, \sigma_N^2 \mathbf{I}_M)$, where \mathbf{I}_M is an $M \times M$ identity matrix. The squared norm $\|\mathbf{n}\|_{\ell_2}^2$ is a Chi-square random variable with mean $\sigma_N^2 M$ and standard deviation $\sigma_N^2 \sqrt{2M}$. With high probability, $\|\mathbf{n}\|_{\ell_2}^2$ cannot exceed the sum of the mean and two times the standard deviation. Thus ϵ in (4) is chosen such that [9]

$$\epsilon^2 = \sigma_N^2 (M + 2\sqrt{2M}). \quad (5)$$

III. A SHANNON-KOTEL'NIKOV MAPPING

In this section, a 1:2 double Archimedes' spiral mapping is described for a Gaussian memoryless source Y with variance σ_Y^2 . Bandwidth expansion is performed by mapping each source sample $y \in \mathbb{R}$ to a two-dimensional channel symbol, which is a point on the double Archimedes' spiral, given by [7]

$$\mathbf{s}(y) = \begin{bmatrix} z_1(y) \\ z_2(y) \end{bmatrix} = \frac{1}{\pi} \begin{bmatrix} \text{sgn}(y)\Delta \varphi(y) \cos \varphi(y) \\ \text{sgn}(y)\Delta \varphi(y) \sin \varphi(y) \end{bmatrix} \quad (6)$$

where $\text{sgn}(\cdot)$ is the signum function, Δ is the radial distance between any two neighboring spiral arms, and $\varphi(y) = \sqrt{6.25}|y|/\Delta$ is a stretching bijective function. For a given channel signal-to-noise ratio (CSNR) defined as P/σ_N^2 , where P and σ_N^2 are the average channel power and noise variance, respectively, the radial distance Δ is optimized to minimize the total distortion by solving the following unconstrained optimization problem

$$\Delta_{\text{opt}} = \arg \min_{\Delta} [\bar{\varepsilon}_{\text{wn}}^2(\Delta) + \bar{\varepsilon}_{\text{th}}^2(\Delta)] \quad (7)$$

where $\bar{\varepsilon}_{\text{wn}}^2$ and $\bar{\varepsilon}_{\text{th}}^2$ are, respectively, the average weak noise and threshold distortion under maximum likelihood (ML) decoding as defined in [7]. For a Gaussian source, the average weak noise distortion is given by [7]

$$\bar{\varepsilon}_{\text{wn}}^2 = \frac{\sigma_N^2}{\alpha^2} \quad (8)$$

where α is a gain factor related to the average channel power constraint P , via

$$P = \frac{1}{2} \int \|\mathbf{s}(\alpha y)\|^2 f_Y(y) dx \quad (9)$$

and $f_Y(y)$ is the probability density function of the source Y . The threshold distortion is approximated by [7]

$$\bar{\varepsilon}_{\text{th}}^2 \approx \left[1 - \text{erf} \left(\frac{\Delta}{2\sqrt{2}\sigma_N} \right) \right] \left[\left(\frac{\pi^4 \eta^2 \Delta^2}{\alpha^2} + 4\sigma_Y^2 \right) \text{erf}(a) - \left(\frac{2\pi^2 \eta \Delta + a\sigma_Y \alpha}{\sqrt{2\pi}\alpha} \right) 8\sigma_Y e^{-\frac{a^2}{2\sigma_Y^2}} + \frac{16\pi^2 \eta \Delta \sigma_Y}{\sqrt{2\pi}\alpha} \right] \quad (10)$$

where $\text{erf}(\cdot)$ is the Gaussian error function, $a = 4\sigma_Y$, and $\eta = 0.16$. Note that (10) is a good approximation at high CSNR levels.

At the receiver side, we use the optimal minimum mean square error (MMSE) decoder instead of the ML decoder used in [7]. MMSE decoding has been shown to achieve a substantial performance improvement over ML decoding at low CSNRs under 2:1 bandwidth reduction [16]. For 1:2 bandwidth expansion, the MMSE decoding rule can be written as follows

$$\begin{aligned} \hat{y}_{\text{MMSE}} &= E[Y|\hat{z}_1, \hat{z}_2] = \int yp(y|\hat{z}_1, \hat{z}_2) dy \\ &= \frac{\int yp(\hat{z}_1, \hat{z}_2|y)p(y) dy}{\int p(\hat{z}_1, \hat{z}_2|y)p(y) dy} \end{aligned} \quad (11)$$

where $\hat{z}_i = z_i + n_i$, $i = 1, 2$, are the received channel outputs. For independent and identically distributed (i.i.d.) Gaussian noise n_1 and n_2 , we have $p(\hat{z}_1, \hat{z}_2|y) = p(\hat{z}_1|y)p(\hat{z}_2|y)$, where

$$p(\hat{z}_i|y) = \frac{1}{\sqrt{2\pi}\sigma_N} e^{-\frac{(\hat{z}_i - z_i(y))^2}{2\sigma_N^2}} \quad i = 1, 2 \quad (12)$$

and $z_i(y)$ is given by (6). Note that (11) is numerically calculated by discretizing y using a uniform quantization step d and calculating the mapped value $(z_1(y), z_2(y))$ for each discretized point. This gives a discretized version of each probability and the integration is simplified to only multiplication and addition operations. Note that this approximation is assumed to be good as long as the cardinality of the discrete set is sufficiently large and d is small in relation to the standard deviation of the channel noise.

In addition to the MMSE decoder, which is optimal in the mean square sense, we propose to use the maximum a-posteriori (MAP) decoder which can be formulated as follows

$$\hat{y}_{\text{MAP}} = \arg \max_y p(y|\hat{z}_1, \hat{z}_2) = \arg \max_y p(y)p(\hat{z}_1, \hat{z}_2|y). \quad (13)$$

To find (13), we discretize the spiral in a similar approach to the MMSE case. Moreover, to make the MMSE/MAP decoder implementation computationally efficient, we devise a decoder based on quantization and table-lookup. This is achieved via uniform quantization of the output of the channel $\hat{\mathbf{z}} \in \mathbb{R}^2$ and looking up the decoded value \hat{y} for each quantization bin in a table.

IV. SYSTEM MODEL

A. System Structure

Consider a group of sensors that is observing a discrete time continuous amplitude source signal $\mathbf{x} \in \mathbb{R}^N$. This observation is assumed to be sparse in some transform basis Ψ . Each sensor encodes its observation and transmits it to the FC over additive white Gaussian noise (AWGN) channels with variance σ_N^2 . The objective is to recover the sensor observations under a mean square error (MSE) fidelity criterion. The proposed system structure is shown in Fig 1.

On the encoder side, the sensors measure the observation using a random measurement matrix Φ . A practical method is

to draw each entry of the measurement matrix independently from a Gaussian distribution (i.e., $[\Phi]_{ij} \sim \mathcal{N}(0, 1/M)$) and then orthogonalize the rows of Φ . The measurement vector is given by

$$\mathbf{y} = \Phi \mathbf{x}, \quad (14)$$

where $\Phi \in \mathbb{R}^{M \times N}$ is the measurement matrix for the CS encoder. Each sample of the measurement vector \mathbf{y} is mapped to a two-dimensional channel space using the double Archimedes' spiral as in (6). It is observed that the measurements from the CS encoder fit well a Gaussian distribution. Hence, the results from Section III are hereafter used; the radial spiral distance Δ is calculated using (7) given the power allocated to the channel input (9) under a total transmission power constraint (see below).

At the receiver side, we use either the MMSE or MAP decoder to obtain the measurement estimate $\hat{\mathbf{y}}$. To recover the original signal, we use BP [13] to solve the ℓ_1 minimization problem in (2), and for comparison also the minimization in (4).

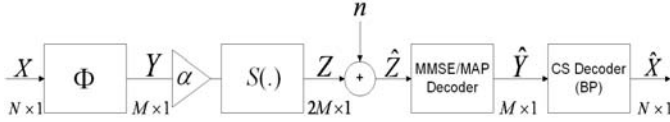


Fig. 1. The proposed system structure.

B. System Optimization

The proposed system is optimized for minimal end-to-end MSE distortion $E[\|\mathbf{x} - \hat{\mathbf{x}}\|^2]$ which is a function of two sources of distortion: D_{CS} from compressed sensing (without lossy transmission) and D_{exp} from channel noise. Given a total transmission power constraint P_{tot} , the aim is to minimize the end-to-end distortion. From CS theory, it is known that the distortion D_{CS} decreases with increasing number of measurements. However, due to the total power constraint, the average power per channel (use) will decrease. This will increase the distortion D_{exp} from bandwidth expansion transmission. Thus, for a given channel quality, we aim to determine the optimal number of measurements which balances these two distortion contributions and results in a minimum overall distortion under the power constraint P_{tot} .

Distortion D_{exp} from dimension expansion is minimized by optimizing Δ using (7). In the CS literature, however, there is not yet an explicit relation between the number of measurements M and the distortion D_{CS} obtained with BP. Thus optimization is done numerically by searching for the number of measurements that minimizes the end-to-end MSE distortion $E[\|\mathbf{x} - \hat{\mathbf{x}}\|^2]$. We create a set of source vectors $\{\mathbf{x}\}$ with signal dimension N . Each source vector is synthesized as $\mathbf{x} = \Psi \mathbf{u}$, where Ψ is the sparsity basis and \mathbf{u} comprises K sparse transform coefficients. There are $\binom{N}{K}$ possible sparsity patterns for \mathbf{u} .¹ Each realization is drawn uniformly from these patterns. For each number of measurements M , we

create a fixed measurement matrix Φ whose entries are drawn from a Gaussian distribution. The set of CS measurement vectors $\{\mathbf{y}\}$ is calculated using (14). For a given noise variance level, (Δ, α) are optimized using (7) under the average power constraint $P = P_{tot}/(2M)$, and a set of noise vectors $\{\mathbf{n}\}$ is created to model the AWGN channel. A 1:2 bandwidth expansion is applied on each component of the measurement vector using the Archimedes' spiral in (6). Then, the measurement estimate $\hat{\mathbf{y}}$ is obtained using MMSE or MAP decoding according to (11) or (13), and BP is used for signal reconstruction according to (2). The end-to-end MSE distortion $E[\|\mathbf{x} - \hat{\mathbf{x}}\|^2]$ is evaluated over the data set $\{\mathbf{x}\}$. We keep increasing the number of measurements M until we observe an increase in the end-to-end distortion. The design suboptimal search algorithm is shown herein.²

Algorithm 1 System Optimization

Data Input: Input a data set $\mathbf{X} = \{\mathbf{x}_1, \dots, \mathbf{x}_T\}$, a channel noise variance σ_N^2 , and a transmission power constraint P_{tot} .
Initialization: Set the number of measurements $M = m$, the incremental step Inc for the number of measurements, and $i = 1$. Set the end-to-end MSE distortion $D^{(0)} = 10^{20}T$, $D^{(1)} = 10^{19}T$, the spiral radial distance $\Delta = \infty$, and the gain factor $\alpha = \infty$.

while $D^{(i)} < D^{(i-1)}$ **do**

$i \leftarrow i + 1$.

Set $\Delta_{opt} \leftarrow \Delta$, $\alpha_{opt} \leftarrow \alpha$, and $D_{opt} \leftarrow D^{(i-1)}$.

Initialize the measurement matrix $\Phi^{(i)}$ as a random Gaussian matrix.

Obtain measurement vector \mathbf{y} for each observation in \mathbf{X} according to (14).

Scale the average channel power constraint according to $P = \frac{P_{tot}}{2M}$, so that power is equally divided between channels.

Optimize (Δ, α) for the given channel noise variance σ_N^2 according to (7) under the power constraint $E[z^2] = P$.

Use the double Archimedes' spiral mapping on \mathbf{y} according to (6) in order to achieve a 1:2 bandwidth expansion.

Decode $\hat{\mathbf{y}}$ using MMSE or MAP decoder according to (11) or (13), and $\hat{\mathbf{x}}$ using BP according to (2).

Calculate numerically $D^{(i)} = E[\|\mathbf{x} - \hat{\mathbf{x}}\|^2]$ over the data set \mathbf{X} .

$M \leftarrow M + Inc$.

end while

$M \leftarrow M - Inc$.

Return $(M, D_{opt}, \Delta_{opt}, \alpha_{opt})$.

In our simulations, we used $T = 30000$, m is set to a small value ($\sim K$), and the incremental step $Inc = 4$. Fig. 2 shows the system signal-to-distortion ratio ($SDR \triangleq E[\|\mathbf{x}\|^2]/E[\|\mathbf{x} - \hat{\mathbf{x}}\|^2]$) as a function of the number of measurements M at different TSNR $\triangleq P_{tot}/\sigma_N^2$ levels.³ Notice that for a fixed

²One source of suboptimality is that the system parameters are not jointly optimized to minimize end-to-end distortion.

³TSNR stands for "total" SNR and is related to CSNR as $TSNR/(2M)$.

¹The sparsity pattern is the set of indices of the nonzero components of \mathbf{u} .

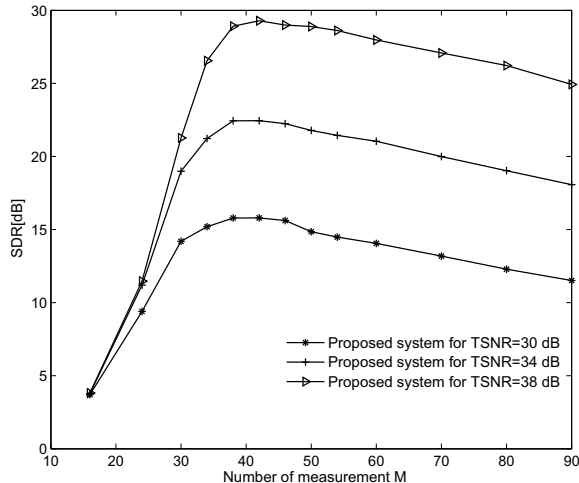


Fig. 2. Performance of the proposed system as a function of number of measurements M with sparsity level $K = 6$ and signal length $N = 100$. For TSNR=38dB, the CSNR [dB] levels at the data points are as follows: [22.9 21.2 20.2 19.7 19.2 18.7 18.4 18 17.6 17.2 16.5 15.9 15.4]. Note that there is a 4dB difference in CSNR levels (as well as in TSNR) between adjacent curves. MMSE decoding and BP are used on the receiver side.

TSNR level, the SDR increases with increasing M until reaching a maximum and then starts to decrease. This occurs because the compressed sensing part performs better as M increases but at the same time, the distortion from channel noise increases. For small M , the CS distortion dominates over the distortion contributions from channel noise. This is clearly shown from the closeness between the SDR curves as well as from the steep increase in SDR of each curve, which is a trend observed in CS theory. As M gets larger beyond a certain level (~ 38), the CS distortion contribution levels off, and the trend in the SDR curves follow the performance of the bandwidth expansion systems. We notice an ~ 7 dB gap in system SDR between neighboring curves. For a given M , there is a 4 dB difference in CSNR between adjacent SDR curves. From Fig. 2, it can be seen that for M between 40-90, the CSNR levels are in the range 8-19 dB. For a 4 dB difference in CSNR in this range, a 1:2 bandwidth expansion system using double Archimedes' spiral gives $6 \sim 8$ dB SDR gain [7]. This explains the ~ 7 dB gap between neighboring curves. Thus the trends in Fig. 2 show clearly the dominance of CS distortion for small M and channel noise for large M .

V. NUMERICAL RESULTS

In this section, we assume a sparse source \mathbf{x} in the discrete cosine transform basis Ψ with signal length $N = 100$. The signal \mathbf{x} is synthetically generated as $\Psi\mathbf{u}$, where there are $K = 6$ nonzero elements in the transform coefficients \mathbf{u} ($\|\mathbf{u}\|_{\ell_0} = K \ll N$). The results presented here are for the case where the nonzero elements u_i are i.i.d. Gaussian with unitary variance and the sparsity pattern is uniformly distributed. We use the spiral mapping, discussed in Section III, to apply 1:2 dimension expansion, and BP to recover the source signal $\hat{\mathbf{x}}$ from the received measurements.

The conventional CS system "CS-BP" which uses BP for signal recovery, does not account for channel noise during reconstruction. However, as mentioned in Section II, there is also a noise-aware version of ℓ_1 minimization in CS theory given by (4) that can recover source signal from noisy measurements [9]. The structure of the reference systems for performance comparison is shown in Fig. 3. We scale the channel input by a gain factor $1/\gamma$ in order to satisfy the average channel power constraint $P = E[(y/\gamma)^2] = 1/\gamma^2 E[y^2]$. At the receiver, we rescale the signal using γ and use either BP or basis pursuit with denoising (BPDN) [13] for signal reconstruction. This is conducted by solving the optimization problem stated in (2) or (4).

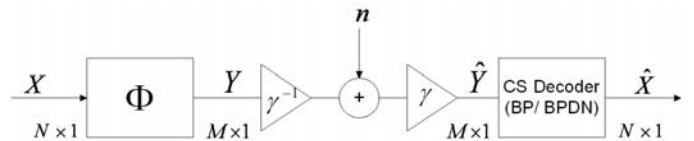


Fig. 3. CS-BP/CS-BPDN structure.

The number of measurements M is optimized for all systems under the total transmission power P_{tot} . This is done using Algorithm 1 for the proposed system, whereas for the reference systems, we search over a range of M to obtain the one that produces the minimum end-to-end distortion. Since the number of measurements varies with the channel noise variance, system SDR is plotted based on TSNR. From Fig. 4, it can be seen that the proposed system "CS-Mapping" outperforms the CS-BP system for all CSNR levels, and "CS-BPDN" from moderate to high CSNRs. At low CSNRs, CS-BPDN gives similar performance as the CS-Mapping. This can be explained by realizing that the 1:2 bandwidth expansion using the double Archimedes' spiral has a similar performance as a linear encoder at low CSNR levels [7]. It can be seen that the SDR from CS-BPDN improves by up to 3 dB when the number of measurements is optimized. However, it needs to be mentioned that the optimized number of measurements (i.e., number of sensors) is around twice as in CS-Mapping. The number of sensors could be a significant cost or complexity variable in WSNs. Notice that the gain from CS-Mapping as well as its gap to CS-BPDN gets more prominent as CSNR increases. Moreover, using MMSE decoding with the proposed system gives at most 0.7 dB gain in SDR over MAP decoding. We also simulate the proposed system when using BPDN instead of BP on the noisy decoded measurement $\hat{\mathbf{y}}$. This gives around 1 dB gain in SDR over the CS-Mapping with BP.⁴ In Fig. 4, the "Best least-square" decoding scheme (applied on the output $\hat{\mathbf{y}}$ of the Shannon-Kotel'nikov decoder) is also plotted as a reference. This decoding scheme requires additional side information as it assumes that the support I (i.e., the nonzero indices in \mathbf{u}) is known a priori by the decoder. Hence, the best way to recover the source signal from the decoded measurement $\hat{\mathbf{y}}$ would be to apply the pseudo-inverse

⁴The number of measurements is optimized for CS-Mapping with BP.

$(\Phi\Psi)_I^\dagger$ on the support, and set the remaining coordinates of \mathbf{u} to zero.

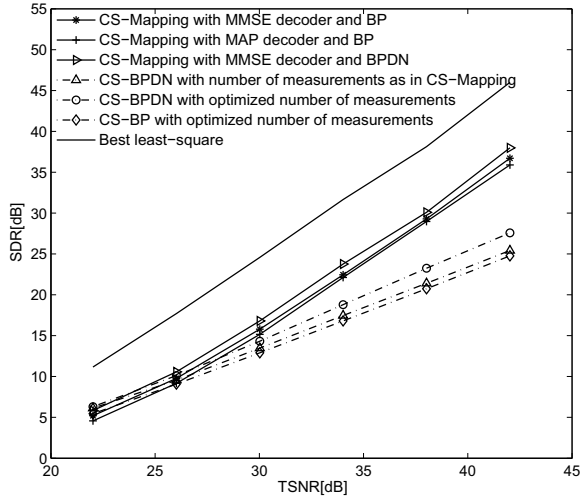


Fig. 4. Performance of CS-Mapping and CS-BPDN with sparsity level $K = 6$ and signal length $N = 100$. The graph is made for $u_i \sim \mathcal{N}(0, 1)$. The number of measurements used by CS-Mapping at the asterisk marks are: [38 38 42 42 42 42], which correspond to the following CSNR[dB] levels: [3.2 7.2 10.7 14.7 18.7 22.7]. The performance of CS-BP is also shown for comparison.

In what follows, we summarize the results of our study (without providing performance curves due to space limitations) of the sensitivity of the CS-Mapping and CS-BPDN system against mismatch in noise level. As in several applications, the encoder has no knowledge on the actual noise variance and a design noise level is assumed. However, the decoder can be designed to operate at the actual noise level provided the receiver can estimate the channel condition. The CS-BPDN system uses an uncoded linear system at the transmitter side which make it less sensitive to noise mismatch. However, we notice a 0.5 dB loss in the CS-BPDN system due to the mismatch in number of measurement between design and actual TSNR levels.

For the proposed system, we notice that for low and moderate design TSNR levels, the mismatch in system SDR is insignificant when the actual TSNR is lower than the design TSNR level (TSNR_D). In contrast, when the actual $\text{TSNR} > \text{TSNR}_D$, a $2 \sim 3$ dB loss in system SDR is noticed for each 4 dB mismatch in TSNR. For high TSNR_D , the proposed system is highly sensitive when the actual (i.e., true) TSNR is lower than TSNR_D . Whereas, when the actual TSNR is greater than TSNR_D , the system SDR does not suffer from leveling-off effect and increases linearly with TSNR—for instance, an increase of 1 dB in TSNR results in a 1 dB increase in SDR. This trend is due to the analog nature of the proposed system in which the threshold effect is not a problem (i.e., the system performance still improves as the noise level decreases [3]). It is important to note that when the proposed system is designed for moderate to high TSNR, it will certainly perform better than the CS-BPDN when actual TSNR is

greater than the designed one. Hence, it might be better to design the proposed system for the highest expected channel noise. But at the same time, the gain from using the proposed system over CS-BPDN will decrease. Finally, it needs to be mentioned that the proposed purely-analog system is quite robust against a reasonable mismatch in channel noise (hybrid digital-analog systems are usually robust against channel noise mismatch [17]).

VI. SUMMARY AND CONCLUSION

In this paper, we have presented a system which combines compressed sensing and bandwidth expansion using Shannon-Kotel'nikov mapping in the presence of noise. The proposed purely-analog system is optimized for minimal end-to-end distortion under a transmission power constraint. We have also proposed to use MAP decoding with Shannon-Kotel'nikov mapping, which demonstrates similar performance as the optimum MMSE decoder. Simulation results have shown that the system outperforms the conventional CS system that assumes noiseless channels and a CS-based system that accounts for channel noise at the decoder.

REFERENCES

- [1] W. Bajwa, J. Haupt, A. Sayeed, and R. Nowak, "Compressive wireless sensing," in *Information Processing in Sensor Networks. The Fifth International Conference*, Nashville, TN, 2006, pp. 134–142.
- [2] C. E. Shannon, "A mathematical theory of communication," *The Bell System Technical Journal*, vol. 27, pp. 379–423, 1948.
- [3] —, "Communication in the presence of noise," in *Proc. IRE*, 1949, pp. 10–21.
- [4] V. A. Kotel'nikov, *The Theory of Optimum Noise Immunity*. New York: McGraw-Hill, 1959.
- [5] S.-Y. Chung, *On the Construction of Some Capacity-Approaching Coding Schemes*. PhD dissertation, Massachusetts Institute of Technology, Sep. 2000.
- [6] T. A. Ramstad, "Shannon mappings for robust communication," *Teletronikk*, vol. 98, no. 1, pp. 114–128, 2002.
- [7] F. Hekland, P. A. Floor, and T. A. Ramstad, "Shannon-Kotel'nikov mappings in joint source-channel coding," *IEEE Trans. Communications*, vol. 57, no. 1, pp. 94–105, Jan 2009.
- [8] A. Kim and F. Hekland, "Dimension reduction and expansion: Distributed source coding in a noisy environment," in *Proc. Data Compression Conference DCC*, Snowbird, Utah, Mar 2008, pp. 332–341.
- [9] E. Candes, J. Romberg, and T. Tao, "Stable signal recovery from incomplete and inaccurate measurements," *Communications on Pure and Applied Mathematics*, vol. 59, no. 8, pp. 1207–1223, 2006.
- [10] D. Donoho, "Compressed sensing," *IEEE Trans. Information Theory*, vol. 52, no. 4, pp. 1289–1306, Apr 2006.
- [11] E. Candes, J. Romberg, and T. Tao, "Robust uncertainty principles: Exact signal reconstruction from highly incomplete frequency information," *IEEE Trans. Information Theory*, vol. 52, no. 2, pp. 489–509, Feb 2006.
- [12] E. Candes and M. B. Wakin, "An introduction to compressive sampling," *IEEE Signal Processing Magazine*, pp. 21–30, Mar. 2008.
- [13] S. Chen, D. Donoho, and M. Saunders, "Atomic decomposition by basis pursuit," *SIAM Journal on Scientific Computing*, vol. 20, no. 1, pp. 31–61, 1998.
- [14] S. Mallat and Z. Zhang, "Matching pursuits with time-frequency dictionaries," *IEEE Trans. Signal Processing*, vol. 41, no. 12, pp. 3397–3415, Dec 1993.
- [15] J. A. Tropp and A. C. Gilbert, "Signal recovery from random measurements via orthogonal matching pursuit," *IEEE Trans. Information Theory*, vol. 53, no. 12, pp. 4655–4666, Dec 2007.
- [16] Y. Hu, J. Garcia-Frias, and M. Lamarca, "Analog joint source channel coding using space-filling curves and MMSE decoding," in *Proc. Data Compression Conference DCC*, Snowbird, Utah, Mar 2009, pp. 103–112.
- [17] M. Skoglund, N. Phamdo, and F. Alajaji, "Hybrid digital-analog source-channel coding for bandwidth compression/expansion," *IEEE Trans. Information Theory*, vol. 52, no. 8, pp. 3757–3763, Aug 2006.